NACA

RESEARCH MEMORANDUM

EFFECT OF SWEEPBACK ON THE LOW-SPEED STATIC AND ROLLING STABILITY DERIVATIVES OF THIN TAPERED WINGS OF ASPECT RATIO 4

By

William Letko and Walter D. Wolhart

Langley Aeronautical Laboratory
Langley Air Force Base, Va.

NATIONAL ADVISORY COMMITTEE
FOR AERONAUTICS

WASHINGTON
August 9, 1949

NATIONAL ADVISORY COMMITTEE FOR AERONAUTICS

RESEARCH MEMORANDUM

EFFECT OF SWEEPBACK ON THE LOW-SPEED STATIC AND ROLLING STABILITY DERIVATIVES OF THIN TAPERED WINGS OF ASPECT RATIO 4

By William Letko and Walter D. Wolhart

SUMMARY

A low-speed investigation was made in the Langley stability tunnel to determine the effect of sweepback on the static and rolling stability derivatives of a series of wings, each of which had a taper ratio of 0.6 and an aspect ratio of 4. The wings were of NACA 65A006 section in planes parallel to the axis of symmetry and had sweepback angles of their quarter-chord line of 3.6°, 32.6°, and 46.7°. Most of the tests were made with the wings in combination with a fuselage.

Results of the investigation indicate that the maximum lift coefficient of the wing-fuselage combinations increased as the angle of sweepback increased. The usual effect of sweepback in reducing the lift-curve slope was confined to the lift-coefficient range between about -0.2 and 0.2 but was less than expected, probably because the usual effect of sweepback was masked by a variable influence of the fuselage. As the sweepback was increased, there was a rearward shift of the aerodynamic center which was greater than indicated by the theory. This shift is believed to be caused by a large destabilizing effect of the fuselage on the 3.6° sweptback wing, while tests showed practically no effect for the 46.7° sweptback wing.

At low lift coefficients the derivative of rolling moment caused by yaw varied linearly with lift coefficient, and the rate of variation was increased with an increase of sweep angle in very much the same manner that is predicted by theory. Because the linear variations were maintained over only very small ranges of lift coefficients for the more highly swept wings, the maximum positive values of the derivatives of rolling moment due to yaw for the 32.6° and 46.7° sweptback wings were smaller than the values of this derivative for the 3.6° sweptback wing at lift coefficients greater than 0.6.

The derivative of yawing moment caused by rolling was either zero or positive through most of the lift-coefficient range for each of the wings tested. At zero lift coefficient there was a decrease of the damping in roll with an increase of sweepback. The values of damping in roll obtained in the rolling-flow test section of the Langley stability tunnel show good agreement with those obtained by free rotation of the models in the Langley 7- by 10-foot tunnel and with the values calculated by Weissinger's theory.

An increase in sweepback caused large reductions in the rolling-moment coefficient and in the wing-tip helix angle resulting from a unit angular deflection of the ailerons about their hinge axis.

INTRODUCTION

The influence of a number of different geometric parameters on the rolling stability derivatives of wings have been investigated in the Langley stability tunnel by means of the rolling-flow technique. (See reference 1.) The investigations have included the effects of aspect ratio and sweep (reference 2), taper ratio (reference 3), dihedral (reference 4), and airfoil section (reference 5). All of the investigations were performed at low Mach numbers and with moderately thick wings. In order to obtain an indication of the rolling characteristics of sweptback wings at higher subsonic speeds, a series of thin wings (NACA 65A006 airfoil section) were tested in the Langley high-speed 7- by 10-foot wind tunnel at Mach numbers from about 0.4 to about 0.9. (See reference 6.) Results were obtained over an angle-of-attack range from 0.3° to 6.5° for the damping-in-roll derivative C_{l_p} and for the aileron effectiveness.

The results of the investigation reported herein were obtained in the rolling-flow test section of the Langley stability tunnel, and the models were those used for the investigation reported in reference 6. The purpose of the present tests was to obtain more complete information, at least at low speeds, on the static and rolling characteristics of the wings and also to obtain a correlation between techniques of the Langley stability tunnel (rolling flow) and the Langley 7- by 10-foot tunnel (free rotation) for determining the damping in roll.

The wings tested were sweptback 3.6°, 32.6°, and 46.7° and had an aspect ratio of 4 and taper ratio of 0.6.

[redacted]

SYMBOLS

The data are presented in the form of standard NACA coefficients of forces and moments which are referred in all cases to the stability axes, with the origin at the quarter-chord point of the mean aerodynamic chord of the models tested. The positive directions of the forces, moments, and angular displacements are shown in figure 1. The coefficients and symbols used herein are defined as follows:

C_L	lift coefficient (L/qS)
C_D	drag coefficient (-X/qS)
C_{D_0}	drag coefficient at zero lift
C_Y	lateral-force coefficient (Y/qS)
C_l	rolling-moment coefficient (L'/qSb)
C_m	pitching-moment coefficient (M/qS$\bar{c}$)
C_n	yawing-moment coefficient (N/qSb)
L	lift
X	longitudinal force
Y	lateral force
L'	rolling moment about X-axis
M	pitching moment about Y-axis
N	yawing moment about Z-axis
q	dynamic pressure $\left(\frac{1}{2}\rho V^2\right)$
ρ	mass density of air
V	free-stream velocity
R	Reynolds number

[redacted]

S wing area

b span of wing, measured perpendicular to plane of symmetry

c chord of wing, measured parallel to plane of symmetry

$\bar{c}$ mean aerodynamic chord $\left(\frac{2}{S}\int_0^{b/2} c^2 dy\right)$

y distance measured perpendicular to the plane of symmetry

a_o slope of section lift curve per radian

A aspect ratio (b^2/S)

α angle of attack measured in plane of symmetry, degrees

δ aileron deflection measured in plane normal to aileron hinge axis, degrees

ψ angle of yaw, degrees

Λ angle of sweepback of quarter-chord line, degrees

$\frac{pb}{2V}$ wing-tip helix angle, radians

p rolling velocity, radians per second

$\left(\frac{pb}{2V}\right)_\delta$ rate of change of wing-tip helix angle per degree of total aileron deflection

C_{l_δ} rate of change of rolling-moment coefficient per degree of total aileron deflection

$$C_{L_\alpha} = \frac{\partial C_L}{\partial \alpha}$$

$$C_{l_\psi} = \frac{\partial C_l}{\partial \psi}$$

[redacted]

$$C_{n_\psi} = \frac{\partial C_n}{\partial \psi}$$

$$C_{Y_\psi} = \frac{\partial C_Y}{\partial \psi}$$

$$C_{l_p} = \frac{\partial C_l}{\partial\left(\frac{pb}{2V}\right)}$$

$$C_{n_p} = \frac{\partial C_n}{\partial\left(\frac{pb}{2V}\right)}$$

$$C_{Y_p} = \frac{\partial C_Y}{\partial\left(\frac{pb}{2V}\right)}$$

APPARATUS AND TESTS

The tests were made in the 6-foot-diameter rolling-flow test section of the Langley stability tunnel. This section is equipped with a motor-driven rotor which imparts a twist to the air stream so that a model mounted rigidly in the tunnel is in a field of flow similar to that which exists about an airplane in rolling flight (reference 1).

The models tested consisted of three wings of NACA 65A006 section in planes parallel to the axis of symmetry. The wings were of aspect ratio 4, taper ratio 0.6, and had sweepback angles of their quarter-chord line of 3.6°, 32.6°, and 46.7°. (See fig. 2.) The wings were equipped with ailerons, each with a span of 40 percent of the wing semispan and a chord equal to 20 percent of the wing chord. Most of the tests were made with the wings in combination with a fuselage. The quarter-chord point of the mean aerodynamic chord of each of the wings was located at the 43-percent point of the fuselage. The principal dimensions of the fuselage are given in figure 3.

The tests were made with the models mounted on a single-strut support (see fig. 4) at the quarter-chord points of their mean

[redacted]

aerodynamic chords. The forces and moments were measured by means of the six-component balance system of the Langley stability tunnel.

Most of the tests were made at a dynamic pressure of 25.1 pounds per square foot which corresponds to a Mach number of 0.13 and a Reynolds number of about 720,000.

The models were tested through an angle-of-attack range from about -4° angle of attack up to and beyond the angle of maximum lift at 0° and $\pm 5^\circ$ angles of yaw in straight flow and at 0° angle of yaw in rolling flow. For the straight-flow tests at 0° angle of yaw, lift, drag, and pitching-moment coefficients are presented. Data obtained in straight flow at $\pm 5^\circ$ angle of yaw and in rolling flow at values of $pb/2V$ of ± 0.0248 and ± 0.0745 were used to obtain derivatives of lateral force, yawing moment, and rolling moments with respect to yaw angle and wing-tip helix angle. In straight-flow tests at zero yaw, rolling moments were obtained over the angle-of-attack range for aileron deflections of $\pm 4^\circ$ and $\pm 8^\circ$, measured in a plane parallel to the plane of symmetry. The corresponding aileron deflections measured in a plane normal to the hinge axis are presented in the following table:

Sweepback Λ (deg)	Aileron deflections parallel to plane of symmetry (deg)	Aileron deflections normal to hinge line (deg)
3.6	±4	±4.01
3.6	±8	±8.02
32.6	±4	±4.45
32.6	±8	±8.89
46.7	±4	±5.44
46.7	±8	±10.83

Some tests of the 46.7° sweptback wing were made without the fuselage. For these tests, the center section of the wing was altered as is shown in figure 5. In straight flow the lift and pitching moment of the wing alone were measured with and without transition strips on the leading edge of the wing at various values of dynamic pressure. The values of Mach number and Reynolds number which correspond to the test dynamic pressures are as follows:

[redacted]

q	M	R
4	0.051	280,000
8	.073	395,000
16	.104	558,000
25	.131	718,000
40	.166	880,000
65	.211	1,116,000

CORRECTIONS

Approximate jet-boundary corrections (similar to those of reference 7) based on unswept-wing theory have been applied to the angle of attack, the drag coefficient, and the rolling-moment coefficient. Corrections for blocking or support-strut tares have not been applied to the results.

RESULTS AND DISCUSSION

Straight-Flow Characteristics

The lift, drag, and pitching-moment characteristics of the three wings, each tested in combination with the fuselage, are presented in figure 6. The pitching-moment results at low lift coefficients indicate that the aerodynamic center moved rearward, from 17.6 percent to 27.0 percent of the mean aerodynamic chord, as the angle of sweepback was increased from 3.6° to 46.7°. The theoretical results given in reference 8 predict almost no change in the aerodynamic-center location of plain wings over this range of sweep angles for the particular aspect ratio and taper ratio of the wings investigated. The differences between theory and experiment probably resulted from the fact that a fuselage was used in the tests.

Because each of the wings was constructed in two semispan segments with mounting blocks at the inboard ends for attachment to a fuselage, true wing-alone characteristics could not be obtained. An attempt to simulate, as nearly as possible, the wing-alone condition was made, however, for the 46.7° sweptback wing. The wing segments were supported by cover plates and the entire root region was faired with balsa wood and clay. (See fig. 5.) Lift and pitching-moment results obtained with this model (wing alone) and with the same wing in

[redacted]

combination with the fuselage are compared in figure 7. The fuselage appeared to have very little effect on the general shapes of the lift and pitching-moment curves or on the aerodynamic-center location determined from the slope of the pitching-moment curve at zero lift. For either the wing alone or the wing-fuselage combination, the aerodynamic center was only about 1 percent of the mean aerodynamic chord behind the location (27 percent of the mean aerodynamic chord) given by the theory of reference 8. Apparently, for the 46.7° sweptback wing the forward location of the wing-fuselage juncture resulted in elimination of the usual unstable pitching-moment contribution of the fuselage. For the wings with smaller sweep angles, the location of the wing-fuselage juncture was farther rearward and, in these cases, the contribution of the fuselage to the pitching-moment characteristics seems to have been a destabilizing effect, as is normally expected. Such an effect (an increase of the unstable pitching-moment contribution of the fuselage with a rearward shift of the wing-fuselage juncture) was found in tests of midwing configurations with straight wings reported in reference 9. The results of reference 9 for a midwing configuration show that as the location of the quarter-chord line of the wing with respect to the fuselage varied from 9 to 44 percent of the fuselage length, the aerodynamic-center location of the configuration varied from 0 to about 6 percent forward of the location for wing alone. For the 3.6° sweptback wing with fuselage, the aerodynamic-center location (17.6 percent of the mean aerodynamic chord) was 7.4 percent forward of the location predicted by the theory of reference 8 for the wing alone.

The results presented in figure 7 show that removal of the fuselage caused a reduction in lift-curve slope (from 0.062 to 0.054) near zero lift; but even with the fuselage removed, the lift-curve slope was slightly higher than the theoretical value (0.052) given in reference 8. The small displacements of the lift and pitching-moment curves for the plain wing, relative to the curves for the wing-fuselage combination, probably resulted from some camber introduced by the fairing of the center section of the wing.

The lift data presented in figure 6 indicate an increase in maximum lift coefficient from 0.80 to 1.02 as the sweepback is increased from 3.6° to 46.7°. This result is in agreement with the findings of another low-scale investigation (reference 10) and has been confirmed for Reynolds numbers as high as 12×10^6 in a recent investigation (unpublished) of wings having geometric properties almost identical to those used for the present investigation.

At lift coefficients below 0.8, the lift curves for the three wings are very nearly the same. Although the theories of references 8 and 11 do predict a reduction in lift-curve slope of plain wings with

increased sweep angle, such a reduction, if it occurs, would be expected to be confined to a very small range of lift coefficients (from about −0.2 to 0.2) for the present models, because above a lift coefficient of 0.2 (somewhere between 0.2 and 0.3) partial separation appears to take place. The separation is indicated from the comparison of the experimental drag curves with the curve obtained by adding the drag at zero lift to the theoretical induced drag for elliptic wings of aspect ratio 4. (See fig. 6.) For each of the wings the experimental drag curve began to depart from the theoretical relation at a lift coefficient somewhere between 0.2 and 0.3. Partial flow separation above this lift coefficient therefore would be expected, which would invalidate the assumptions of the theory used to calculate the lift-curve slope. According to previous experience (see fig. 4 of reference 2, for example), the onset of flow separation, as indicated by an increase in the quantity $\left(C_D - \frac{C_L^2}{\pi A}\right)$, generally is accompanied by an increase in lift-curve slope for sweptback wings and a decrease in lift-curve slope for unswept wings. At the higher lift coefficients, therefore, sweptback wings may have lift-curve slopes as high or even higher than those of unswept wings of the same aspect ratio.

The results in figure 6 do not show an effect of sweep on lift-curve slope as large as was expected (on basis of references 8 and 11) for these models, even at the low lift coefficients. This difference may have resulted in part from the use of the fuselage. As has already been pointed out, removal of the fuselage caused a reduction in lift-curve slope from 0.062 to 0.054 for the 46.7° sweptback wing. Tests with straight wings (reference 9 and comparison of references 12 and 13) and tests of a 42° sweptback wing (reference 14) have indicated that the effect on the lift-curve slope of the addition of a fuselage of circular cross section depends, at least partly, on the wing geometry and on the longitudinal position of the wing-fuselage juncture. It is probable, therefore, that the usual effect of sweepback on the lift-curve slope was partially masked by a variable influence of the fuselage.

In order to determine how critically the wing characteristics were affected by changes in Reynolds number, in the range for which most of the tests had to be run, tests were made at various Reynolds numbers with and without transition strips on the leading edge of the wings. Plots to show the effect of transition strips and Reynolds numbers on the lift-curve slope and pitching-moment slope of the 46.7° sweptback wing tested alone are presented as figures 8 and 9, respectively. A summary of these results is presented in figure 10, which shows the variation of lift-curve slope and the variation of the location of the aerodynamic center with Reynolds number. Also presented in figure 10 is the theoretical value for lift-curve slope

[redacted]

and the value for the location of the aerodynamic center as presented in reference 8. The effect of increasing Reynolds number was to decrease the lift-curve slope and to cause a forward shift of the aerodynamic center. The effect on the lift-curve slope and on the aerodynamic-center location of increasing the Reynolds number from 280,000 to 1,116,000 was approximately equivalent to fixing the transition at the nose of the airfoil. The fact that the characteristics of the wing were almost the same with transition strips, either on or off, at a Reynolds number of 1,116,000, is an indication that further increases in Reynolds number would not be particularly important, at least for the present test condition of surface smoothness and air-stream turbulence. Under conditions of extremely low turbulence and with highly polished wing surfaces, the results obtained with transition strips off probably would not approach those with strips on until a Reynolds number considerably higher than 1,116,000 had been attained. (See reference 15.)

The effect of sweepback on the static lateral stability characteristics is shown in figure 11. At low lift coefficients the rate of change of C_{l_ψ} with lift coefficient decreases as the sweep is decreased. For the 32.6° and 46.7° sweptback wings the values of C_{l_ψ} increase linearly for only a small range of lift coefficients after which there is an abrupt change in the initial trends, probably as a result of early partial stalling, mentioned previously. The 32.6° and 46.7° sweptback wings attain relatively small positive values of C_{l_ψ} (less than the values obtained for the unswept wing at lift coefficients greater than 0.6). There is little effect of sweepback on the values of C_{n_ψ} and C_{Y_ψ}. The fuselage causes large positive contributions to both C_{n_ψ} and C_{Y_ψ}. This contribution is shown in figure 12, which compares the values obtained for the 46.7° sweptback-wing and fuselage combination with those for the faired wing alone. Removing the fuselage causes, for the 46.7° sweptback wing, a small change in the variation of C_{l_ψ} with lift coefficient for low coefficients but has no effect on the maximum positive value of C_{l_ψ} attained with the combination.

Rolling-Flow Characteristics

The variations of the rolling derivatives C_{Y_p}, C_{n_p}, and C_{l_p} with lift coefficient are presented in figure 13. As was explained in the

section entitled "Apparatus and Tests," measurements of forces and moments were obtained at four values of $pb/2V$. The derivatives were obtained from the average slopes of the data when plotted against $pb/2V$. In general, the slopes of the curves were well defined and the scatter of tests points was of the order of that obtained in other investigations which have utilized the rolling-flow technique. (See reference 7, for example.)

At low lift coefficients the results presented in figure 13 for the derivatives of lateral force caused by rolling C_{Y_p} are in qualitative agreement with the approximate theory of reference 11 in that this derivative varied linearly with lift coefficient and the rate of variation increased with an increase in sweep angle. In general, C_{Y_p} maintained its initial linear variation over about the same range of lift coefficients as the derivative C_{l_ψ}.

The derivative of yawing moment caused by rolling C_{n_p} was found to be either zero or positive from a lift coefficient of -0.2 to approximately the maximum positive lift coefficient for each of the wings tested. The approximate theory of reference 11, which is based on potential-flow considerations, indicates an initial negative slope of C_{n_p} with C_L; however, this initial trend would be expected to be maintained only over the range of lift coefficients for which the total drag is approximately equal to the drag at zero lift plus the induced drag. (See reference 2.) As is indicated by the drag data of figure 6, this condition is satisfied only up to lift coefficients of about 0.2 or 0.3. At such low lift coefficients the magnitudes of the theoretical values of the yawing moment due to rolling probably are within the experimental accuracy of the measurements and, therefore, no initial negative slope could be detected.

The experimental results for the derivative C_{n_p} are compared in figure 14 with results calculated by a method (presented in reference 2) which includes consideration of the drag measured under straight-flow conditions. In general, fair agreement is obtained, although the predicted values of C_{n_p} at high lift coefficients are too highly positive for the 3.6° and 32.6° sweptback wings. In reference 2, through analysis of experimental data, the increment of C_{n_p} due to profile drag was found to be proportional to the slope of the curve of profile drag plotted against angle of attack, and the constant of proportionality was found to vary with aspect ratio but to be essentially independent of the sweep angle. The comparison presented

in figure 14 indicates that the constant of proportionality probably should be somewhat lower than that given in reference 2 for wings having sweep angles less than about 45°.

At low lift coefficients the negative value of C_{l_p} (fig. 13) of the wing–fuselage combination decreases as the sweep is increased. At some lift coefficient which decreases with an increase in sweep, there is a sudden increase in C_{l_p}. The magnitude of the increase is greatest for the wing with the largest sweep. At the higher lift coefficients the damping decreases for all three wings.

A comparison of values of C_{l_p} obtained by the rolling-flow technique of the Langley stability tunnel with those obtained from the free-rotation tests of the models in the Langley 7- by 10-foot tunnel (reference 6) is presented in figure 15. In general, the variation of C_{l_p} with lift coefficient is similar, and the values of C_{l_p} are in good agreement. The Langley 7- by 10-foot tunnel results are slightly higher, but this difference can be attributed almost entirely to the difference in Mach number of the tests, as is indicated in figure 16, which compares experimental results obtained by the two techniques with theoretical results (from reference 16) corresponding to the two test Mach numbers. The difference between the two theoretical curves is almost exactly equal to the difference between the two experimental curves. Both experimental techniques yield values that are consistently larger than the theoretical values, although the experimental variation of C_{l_p} with sweep angle is in good agreement with theory.

The 46.7° sweptback wing was also tested in rolling flow with the fuselage removed. The effect on C_{Y_p}, C_{n_p}, and C_{l_p} of removing the fuselage was small. (See fig. 17.) The values of C_{l_p} obtained with the wing alone were slightly larger than those obtained for the combination, although the slope of the lift curve for wing alone was lower than that obtained with the combination. A similar result was obtained in the tests reported in reference 17 which gives as a possible explanation the fact that the loading on the fuselage during roll would act normal to the surface of the circular cross-section fuselage and would contribute little to the damping in roll.

[redacted]

Aileron Characteristics

The effects of sweepback on the aileron rolling-moment-effectiveness parameter C_{l_δ} and on the rolling-effectiveness parameter $(pb/2V)_\delta$ are shown in figure 18. The values of C_{l_δ} were determined in straight flow and the values of $(pb/2V)_\delta$ were determined from the relation

$$\left(\frac{pb}{2V}\right)_\delta = \frac{C_{l_\delta}}{C_{l_p}}$$

where C_{l_p} is obtained from figure 13 and represents the damping of the wing with ailerons neutral. The values of $(pb/2V)_\delta$ presented in figure 18, therefore, neglect any possible effect of aileron deflection on the damping in roll or of rolling on aileron effectiveness. Previous experience has indicated, however, that such effects are negligible, except for very large aileron deflections or for angles of attack near the maximum lift coefficient.

Results obtained for the parameters C_{l_δ} and $(pb/2V)_\delta$ depend, of course, on the particular convention used in defining the aileron deflection δ. In the present paper, δ is measured in a plane perpendicular to the aileron hinge axis and, therefore, a given value of δ represents a constant angular rotation of the aileron about its hinge axis regardless of the sweep angle of the wing. With this convention, an increase in sweep angle is found to produce large reductions in both C_{l_δ} and $(pb/2V)_\delta$. (See fig. 18.) According to an alternate convention, the deflection δ is measured in the plane of symmetry and, therefore, a constant value of δ corresponds to an increasing angular rotation of the aileron about the hinge line as the wing sweep angle is increased. When the latter convention is used, the effect of sweepback on the parameters C_{l_δ} and $(pb/2V)_\delta$ is found to be considerably smaller than that indicated in figure 18.

A comparison of figures 18 and 13 shows that for the three wings investigated the variation of C_{l_δ} with lift coefficient is small relative to the variation of C_{l_p} with lift coefficient. The resulting variation of the rolling-effectiveness parameter $(pb/2V)_\delta$,

therefore, is determined primarily by C_{l_p}. All of the wings show reductions in rolling effectiveness as the lift coefficient is increased up to about 0.5. In the case of the 46.7° sweptback wing, this reduction amounts to about 40 percent of the value at zero lift. At higher lift coefficients $(pb/2V)_\delta$ increases for all of the wings because C_{l_p} decreases more rapidly than C_{l_δ}. The values of $(pb/2V)_\delta$ presented in figure 18, however, (as previously mentioned) neglect any possible effect of aileron deflection on the damping in roll or of rolling on aileron effectiveness.

CONCLUSIONS

An investigation made in the Langley stability tunnel of a series of thin sweptback wings of aspect ratio 4, each tested in combination with a fuselage, indicates the following conclusions:

1. The maximum lift coefficient of the wing-fuselage combinations increased as the angle of sweepback increased. At lift coefficients below 0.8, the lift curves were very nearly the same for all three models. The usual effect of sweepback in reducing the lift-curve slope appeared to be confined to the lift-coefficient range between about −0.2 and 0.2 but was less than was expected, probably because the usual effect of sweepback was masked by a variable influence of the fuselage.

2. The aerodynamic center at low lift coefficients moved rearward from 17.6 percent to 27.0 percent of the mean aerodynamic chord as the sweep angle was increased from 3.6° to 46.7°. This rearward shift was considerably larger than that indicated by theory for plain wings and appears to have been caused by a variable contribution of the fuselage. For the 46.7° sweptback wing, tests showed that the fuselage had almost no effect on the aerodynamic center; but for the 3.6° sweptback wing, the fuselage is believed to have a destabilizing effect, as is usually expected.

3. At low lift coefficients the derivative of rolling moment due to yaw varied linearly with lift coefficient, and the rate of variation increased with an increase in sweep angle in very much the manner that is predicted by theory. The linear variations were maintained over only very small ranges of lift coefficient for the more highly swept wings; however as a result, the maximum positive values of the derivative of rolling moment due to yaw for the 32.6° and 46.7° sweptback wings were smaller than the values of this derivative for the 3.6° sweptback wing at lift coefficients greater than 0.6.

[redacted]

4. The derivative of yawing moment due to rolling was either zero or positive through most of the lift-coefficient range for each of the wings tested.

5. At zero lift coefficient there is a decrease in damping in roll with an increase of sweepback. The values obtained in the Langley stability tunnel by the rolling-flow technique show good agreement throughout the sweep range with those obtained by free rotation of the models in the Langley 7- by 10-foot tunnel and with those calculated by Weissinger's theory.

6. An increase in sweepback caused large reductions in the rolling moment and in the wing-tip helix angle resulting from a unit angular deflection of the ailerons about their hinge axes. For the 46.7° swept-back wing, the rate of variation of wing-tip helix angle with aileron deflection decreased by about 40 percent as the lift coefficient increased from 0 to 0.5 but then increased slightly with a further increase in lift coefficient.

Langley Aeronautical Laboratory
National Advisory Committee for Aeronautics
Langley Air Force Base, Va.

[redacted]

REFERENCES

1. MacLachlan, Robert, and Letko, William: Correlation of Two Experimental Methods of Determining the Rolling Characteristics of Unswept Wings. NACA TN 1309, 1947.

2. Goodman, Alex, and Fisher, Lewis R.: Investigation at Low Speeds of the Effect of Aspect Ratio and Sweep on Rolling Stability Derivatives of Untapered Wings. NACA TN 1835, 1949.

3. Brewer, Jack D., and Fisher, Lewis R.: Effect of Taper Ratio on the Low-Speed Rolling Stability Derivatives of Swept and Unswept Wings of Aspect Ratio 2.61. NACA RM L8H18, 1948.

4. Queijo, M. J., and Jaquet, Byron M.: Calculated Effects of Geometric Dihedral on the Low-Speed Rolling Derivatives of Swept Wings. NACA TN 1732, 1948.

5. Letko, William, and Brewer, Jack D.: Effect of Airfoil Profile of Symmetrical Sections on the Low-Speed Rolling Derivatives of 45° Sweptback-Wing Models of Aspect Ratio 2.61. NACA RM L8L31a, 1949.

6. Kuhn, Richard E., and Myers, Boyd C., II: Effects of Mach Number and Sweep on the Damping-in-Roll Characteristics of Wings of Aspect Ratio 4. NACA RM L9E10, 1949.

7. Feigenbaum, David, and Goodman, Alex: Preliminary Investigation at Low Speeds of Swept Wings in Rolling Flow. NACA RM L7E09, 1947.

8. DeYoung, John: Theoretical Additional Span Loading Characteristics of Wings with Arbitrary Sweep, Aspect Ratio, and Taper Ratio. NACA TN 1491, 1947.

9. Jacobs, Eastman N., and Ward, Kenneth E.: Interference of Wing and Fuselage from Tests of 209 Combinations in the N.A.C.A. Variable-Density Tunnel. NACA Rep. 540, 1935.

10. Goodman, Alex, and Brewer, Jack D.: Investigation at Low Speeds of the Effect of Aspect Ratio and Sweep on Static and Yawing Stability Derivatives of Untapered Wings. NACA TN 1669, 1948.

11. Toll, Thomas A., and Queijo, M. J.: Approximate Relations and Charts for Low-Speed Stability Derivatives of Swept Wings. NACA TN 1581, 1948.

[redacted]

12. Bamber, M. J., and House, R. O.: Wind-Tunnel Investigation of Effect of Yaw on Lateral-Stability Characteristics. I – Four N.A.C.A. 23012 Wings of Various Plan Forms with and without Dihedral. NACA TN 703, 1939.

13. Recant, Isidore G., and Wallace, Arthur R.: Wind-Tunnel Investigation of Effect of Yaw on Lateral-Stability Characteristics. III – Symmetrically Tapered Wing at Various Positions on Circular Fuselage with and without a Vertical Tail. NACA TN 825, 1941.

14. Salmi, Reino J., Conner, D. William, and Graham, Robert R.: Effects of a Fuselage on the Aerodynamic Characteristics of a 42° Sweptback Wing at Reynolds Numbers to 8,000,000. NACA RM L7E13, 1947.

15. Neely, Robert H., and Conner, D. William: Aerodynamic Characteristics of a 42° Swept-Back Wing with Aspect Ratio 4 and NACA 64_1-112 Airfoil Sections at Reynolds Numbers from 1,700,000 to 9,500,000. NACA RM L7D14, 1947.

16. Bird, John D.: Some Theoretical Low-Speed Span Loading Characteristics of Swept Wings in Roll and Sideslip. NACA TN 1839, 1949.

17. Bird, John D., Lichtenstein, Jacob H., and Jaquet, Byron M.: Investigation of the Influence of Fuselage and Tail Surfaces on Low-Speed Static Stability and Rolling Characteristics of a Swept-Wing Model. NACA RM L7H15, 1947.

[redacted]

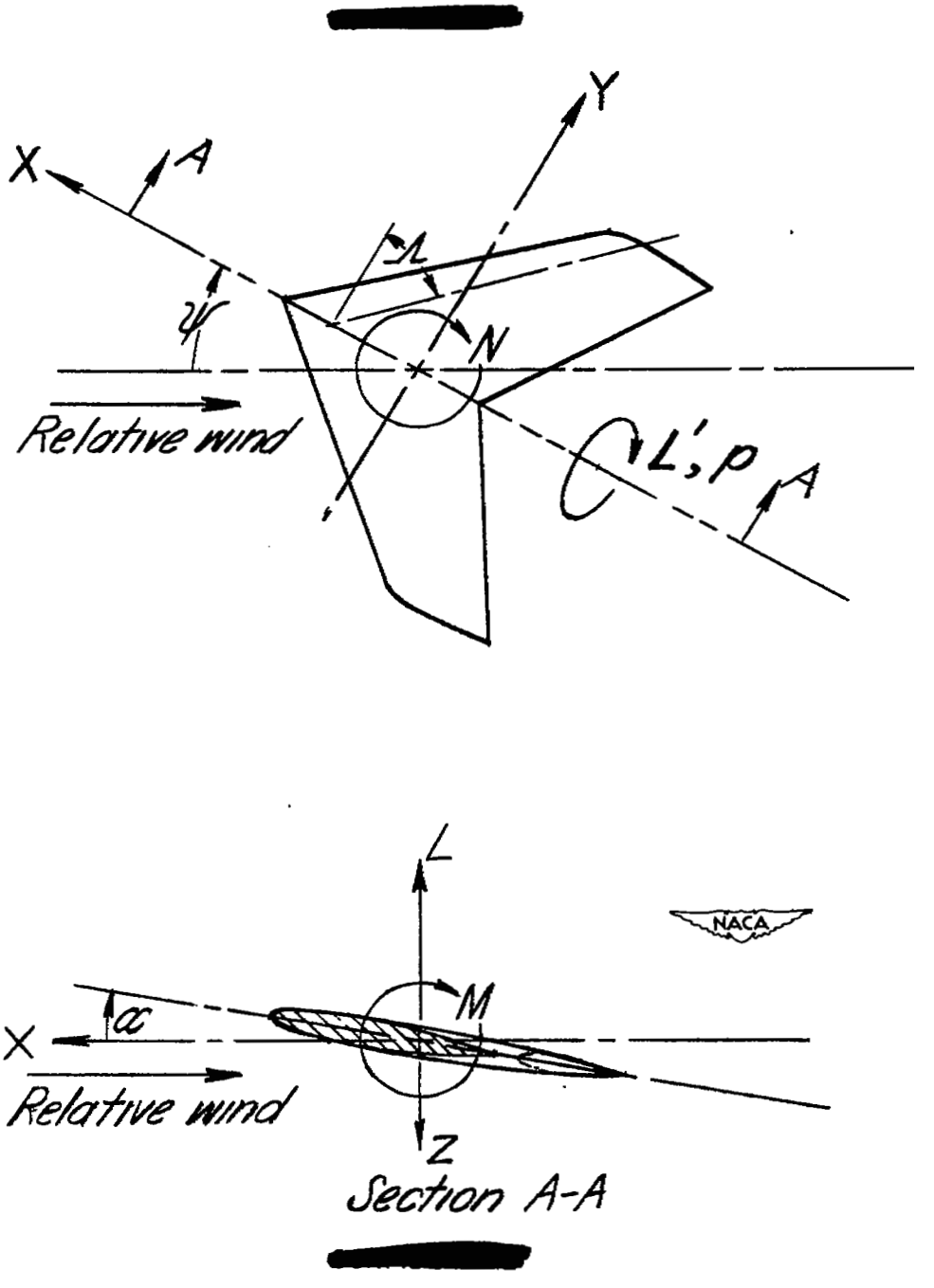

Figure 1.— System of axes used. Arrows indicate positive direction of angles, forces, and moments.

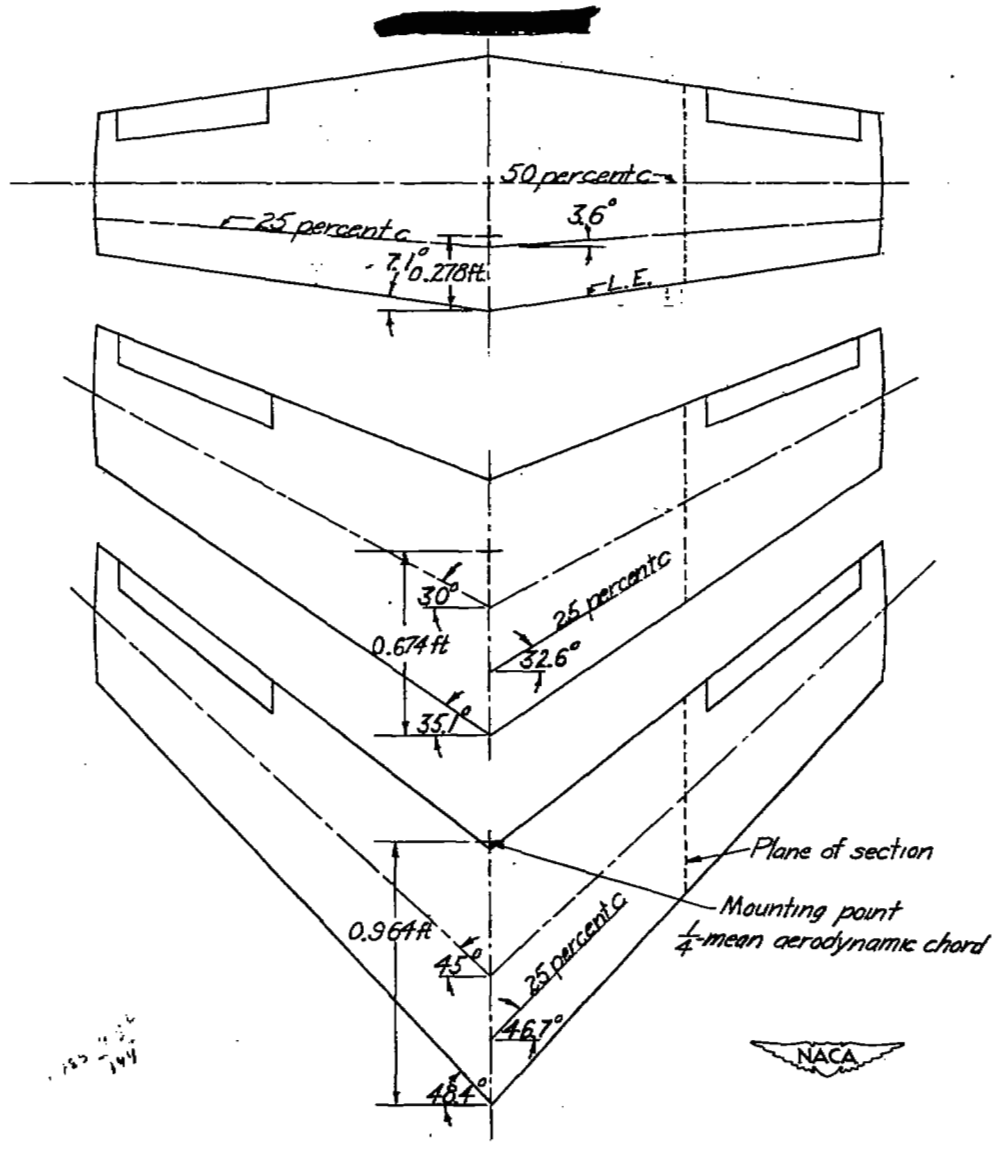

Wing:		Aileron:	
Area, sq ft	2.25	Type	True contour, sealed gap
Aspect ratio	4.0	Chord, percent c	20
Airfoil section	NACA 65A006	Span, percent b/2	40
Span, ft	3.0	Inboard station, percent b/2	55
Mean aerodynamic chord, ft	0.765	Outboard station, percent b/2	95
Taper ratio	0.60		
Root chord, ft	0.938		
Tip chord, ft	0.563		

Figure 2.– Sketch and dimensions of wings tested.

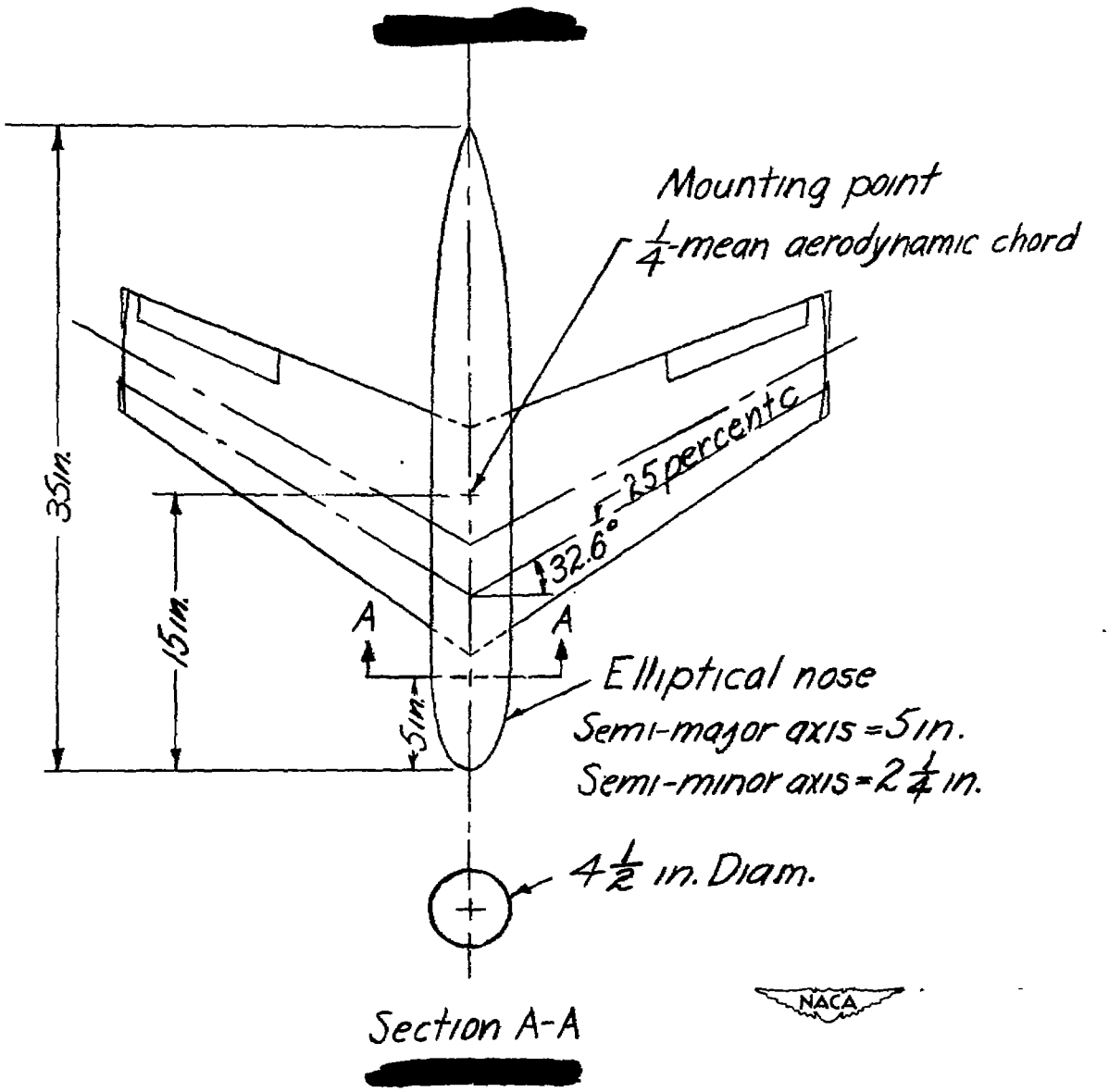

Figure 3.– Sketch of the fuselage and 32.6° sweptback wing giving the principal dimensions of the fuselage.

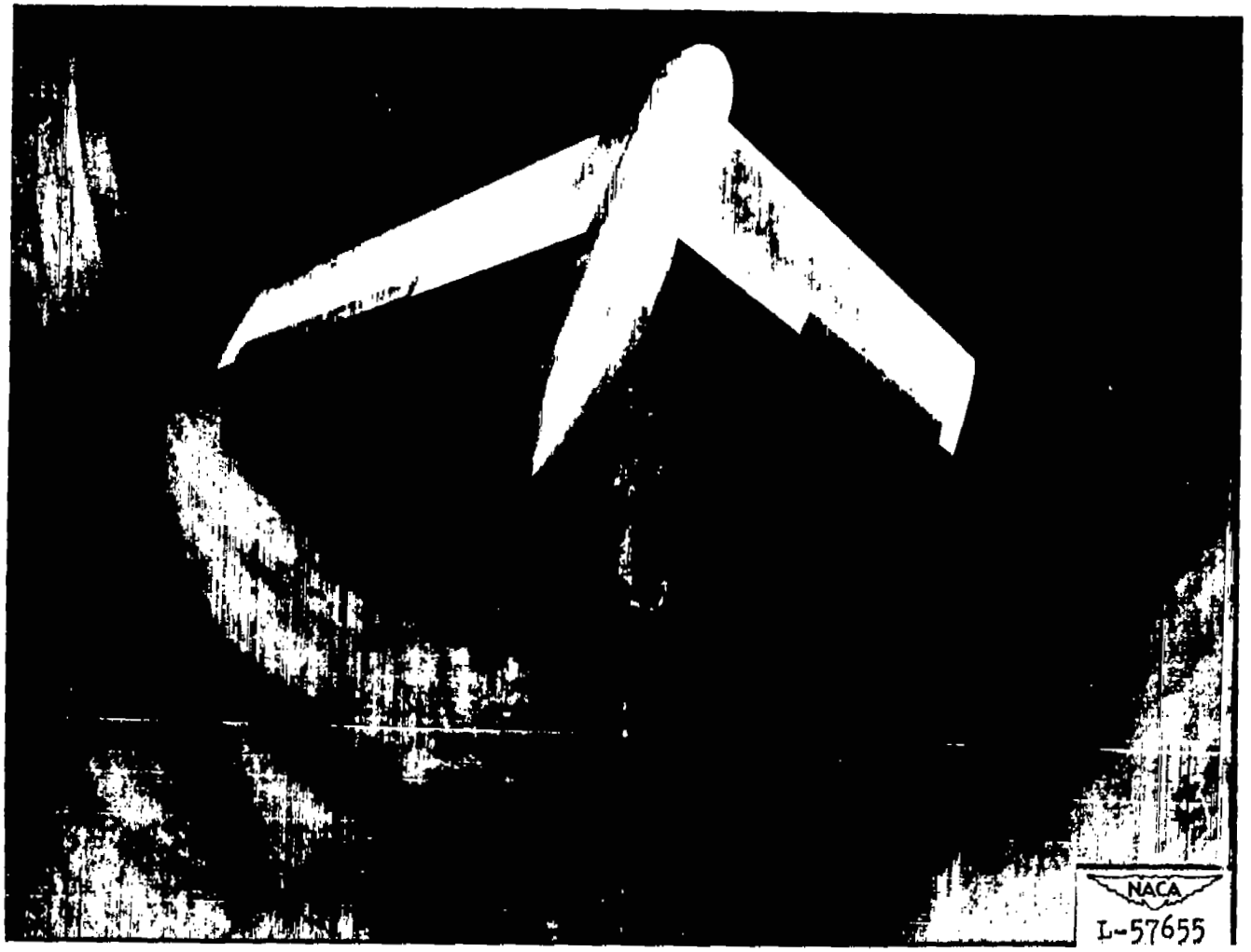

Figure 4.– The 46.7° sweptback wing with fuselage mounted in the rolling-flow section of the stability tunnel.

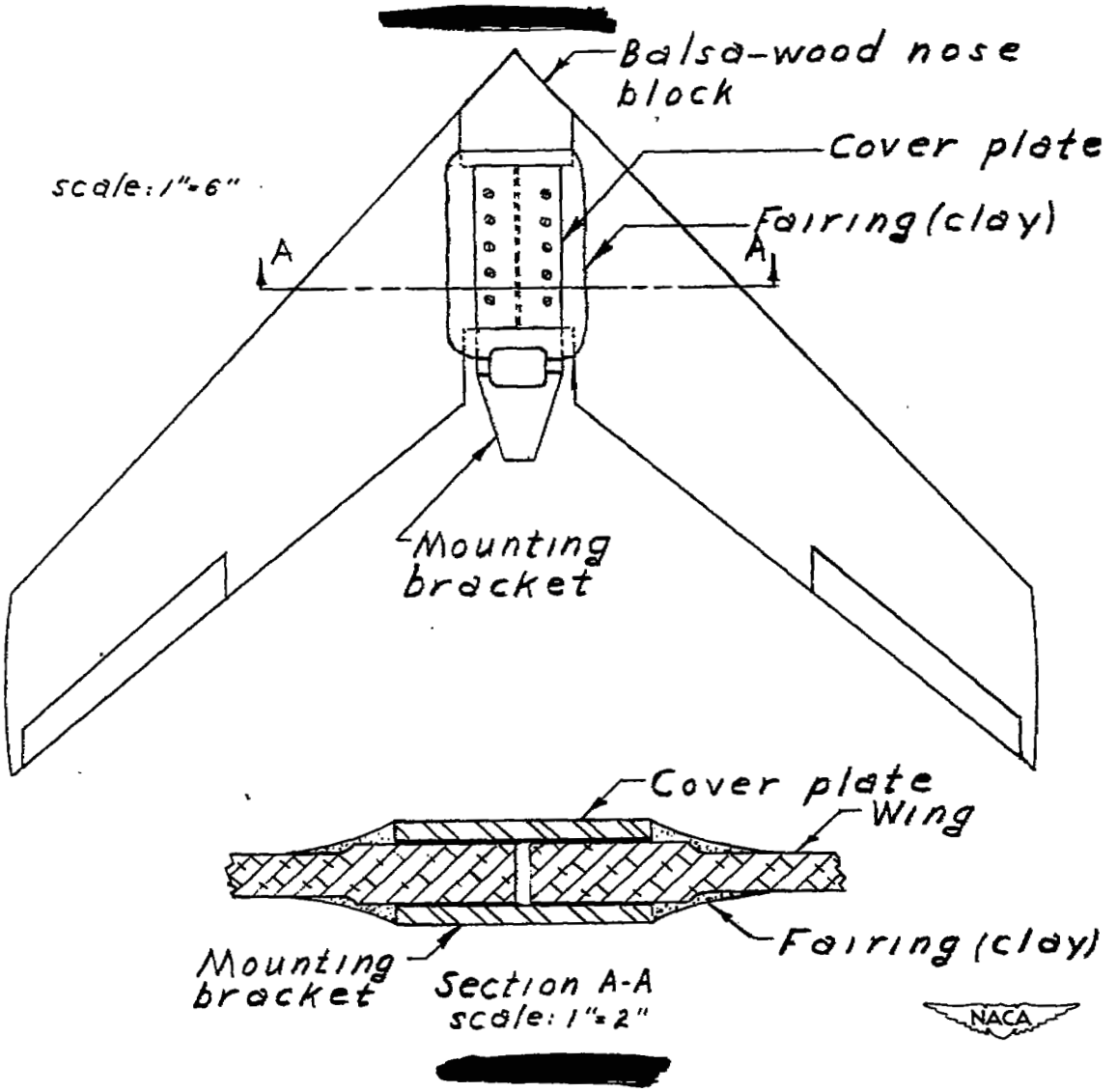

Figure 5.– Sketch of the 46.7° sweptback wing showing modifications made to the wing for tests without fuselage.

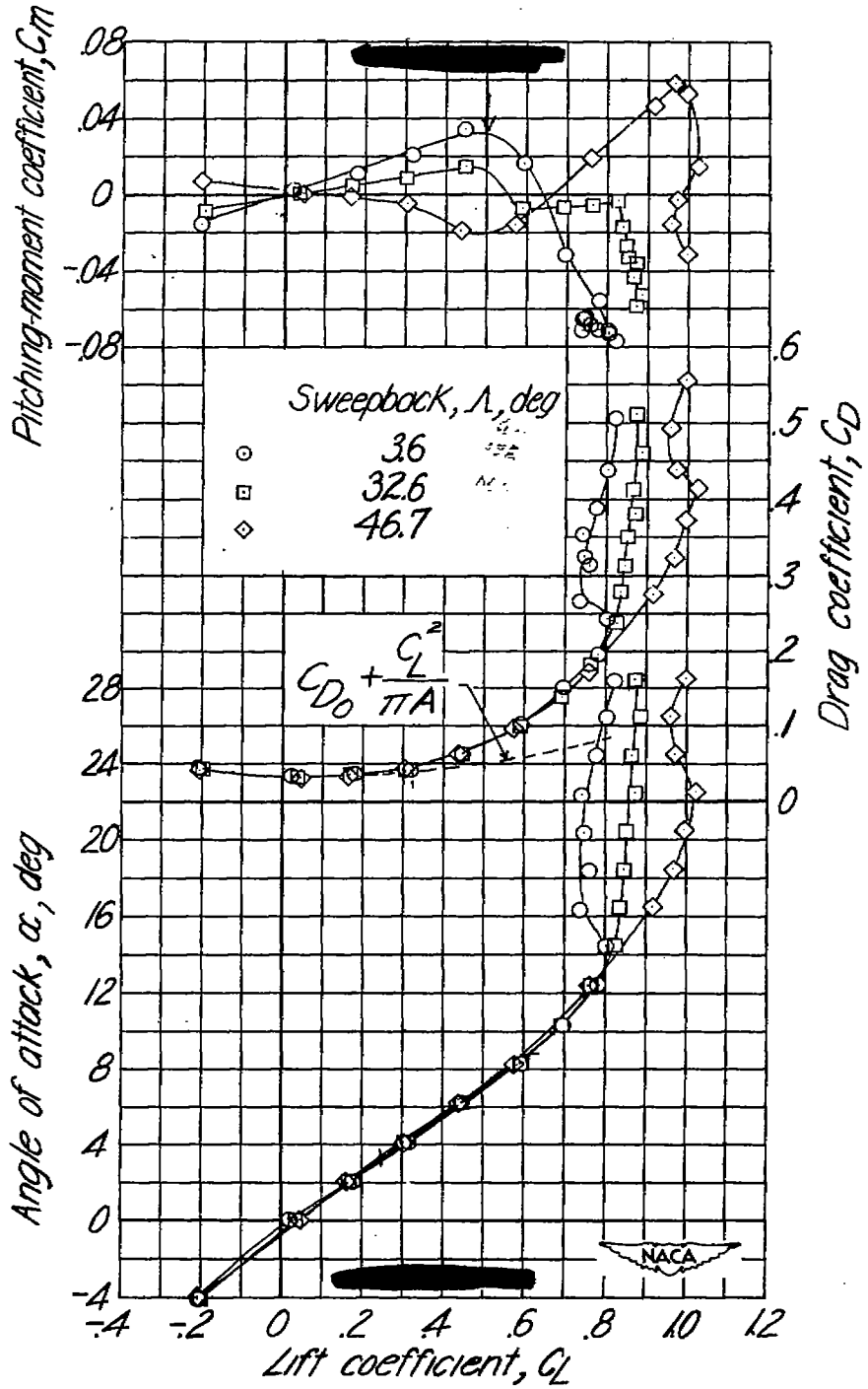

Figure 6.– Variation of the drag and pitching-moment coefficients and angle of attack with lift coefficient for wings tested with a fuselage.

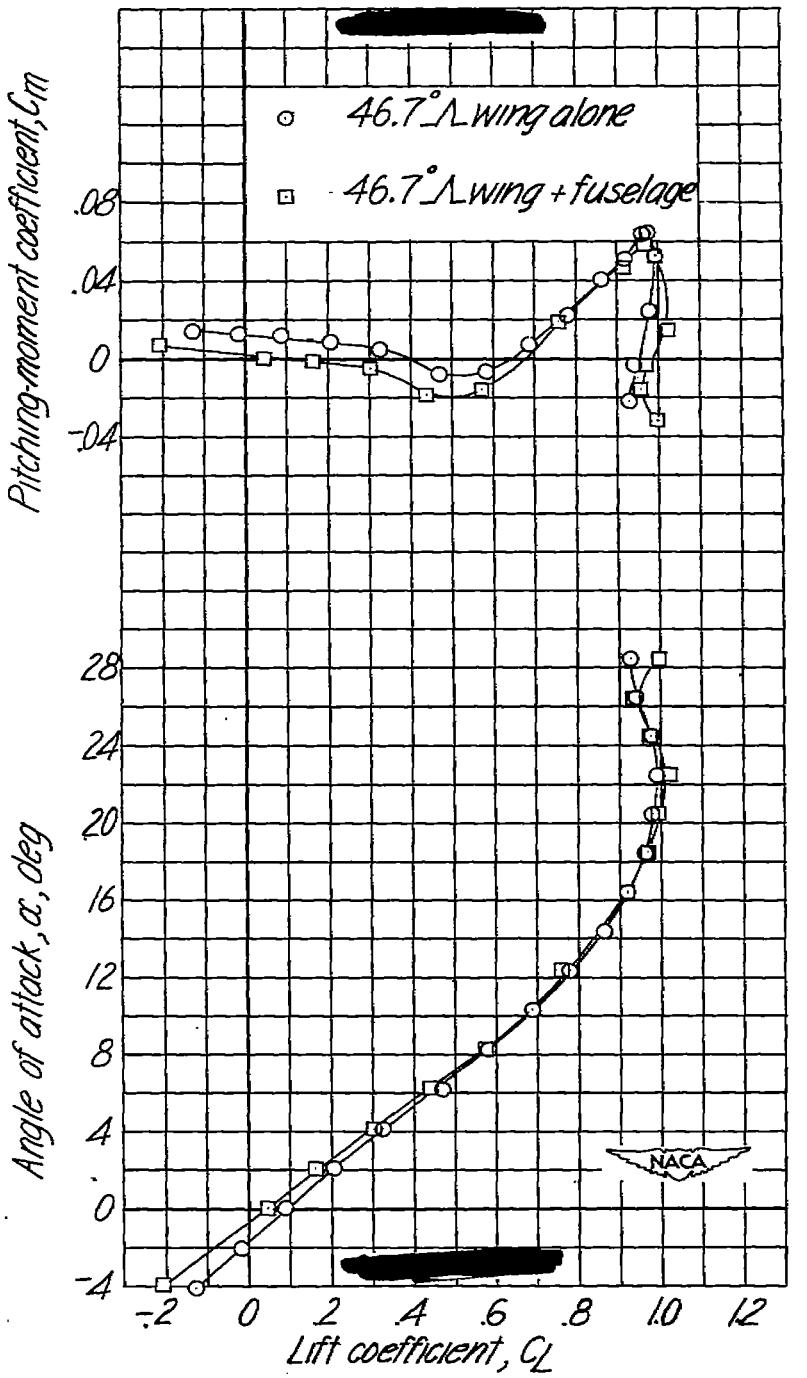

Figure 7.– Variation of the pitching-moment coefficient and the angle of attack with lift coefficient for the 46.7° sweptback wing alone and for the 46.7° sweptback wing in combination with the fuselage.

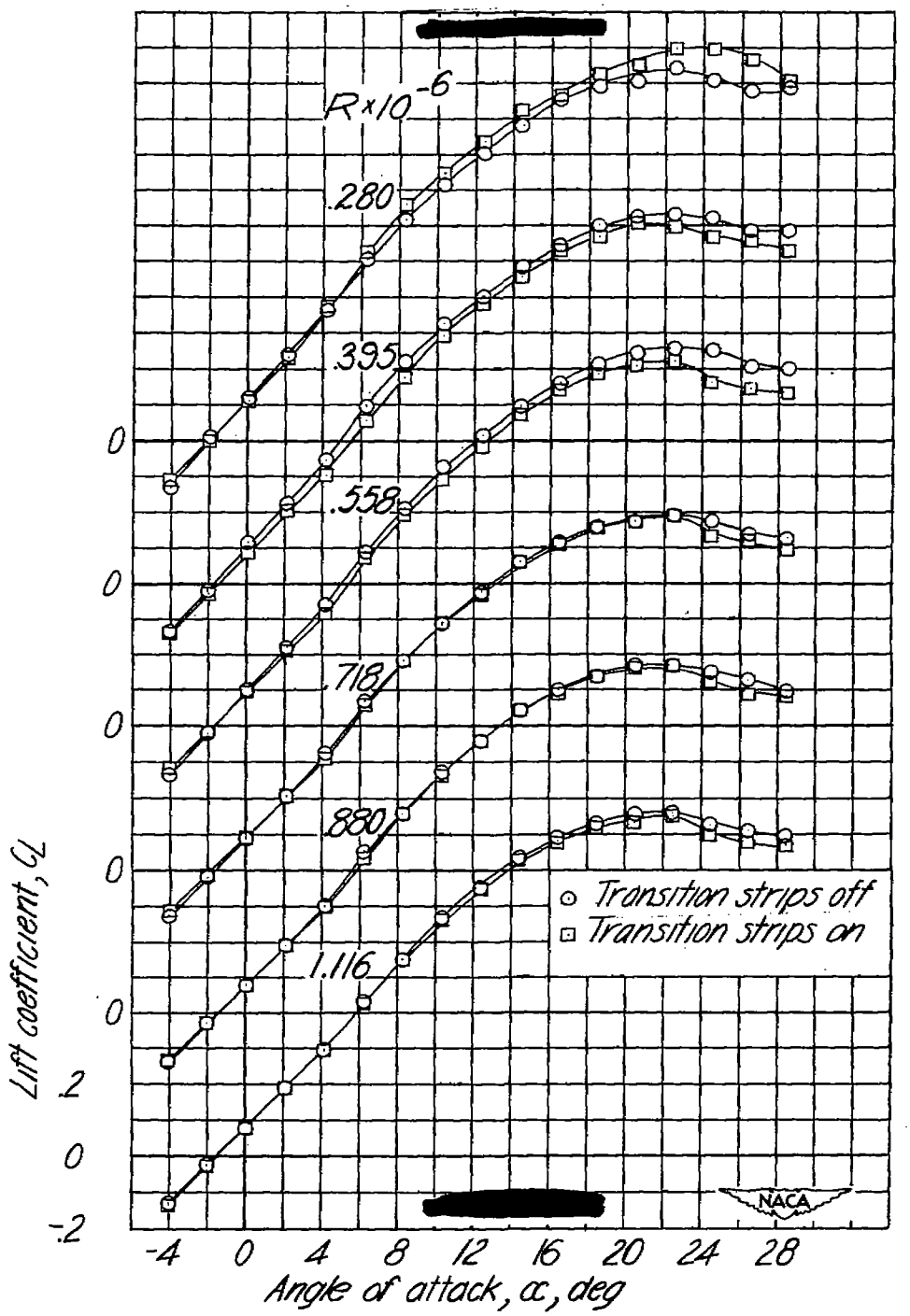

Figure 8.— Variation of the lift coefficient with angle of attack of the 46.7° sweptback wing alone for various values of Reynolds number with and without transition strips on wing leading edge.

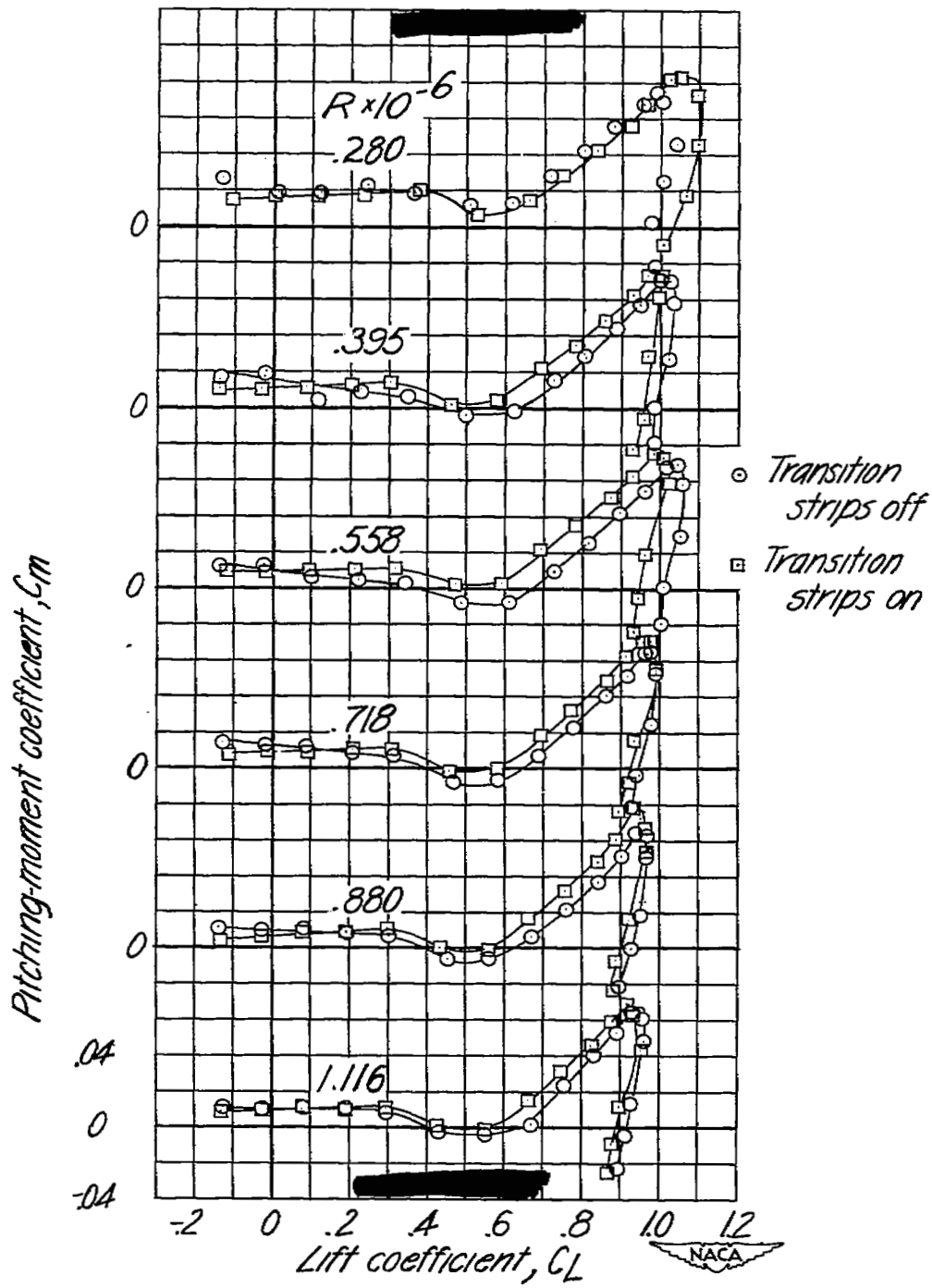

Figure 9.– Variation of the pitching-moment coefficient with lift coefficient of the 46.7° sweptback wing alone for various values of Reynolds number with and without transition strips on wing leading edge.

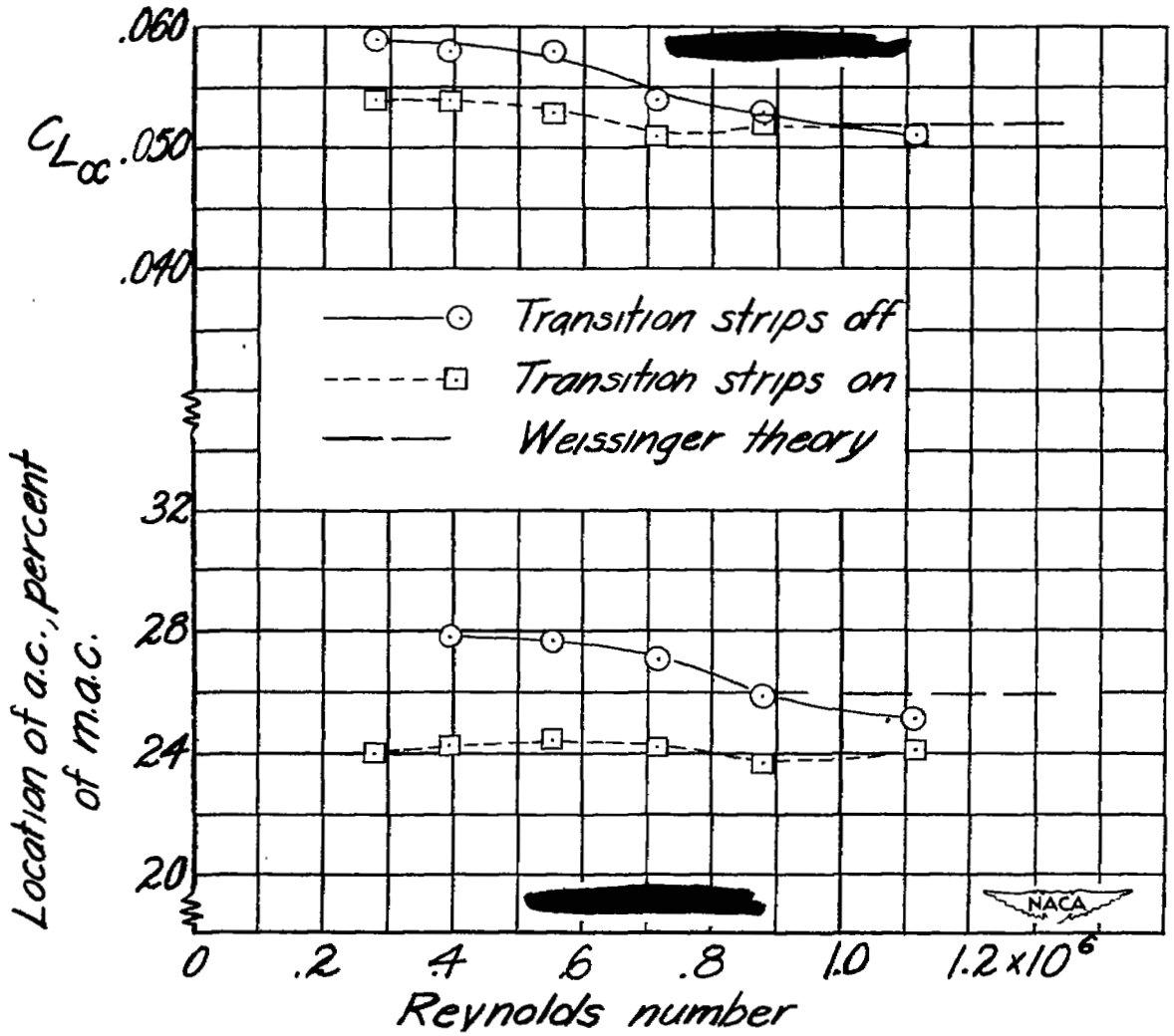

Figure 10.– Effect of transition strips and Reynolds number on the lift-curve slope and location of the aerodynamic center for the 46.7° sweptback wing alone.

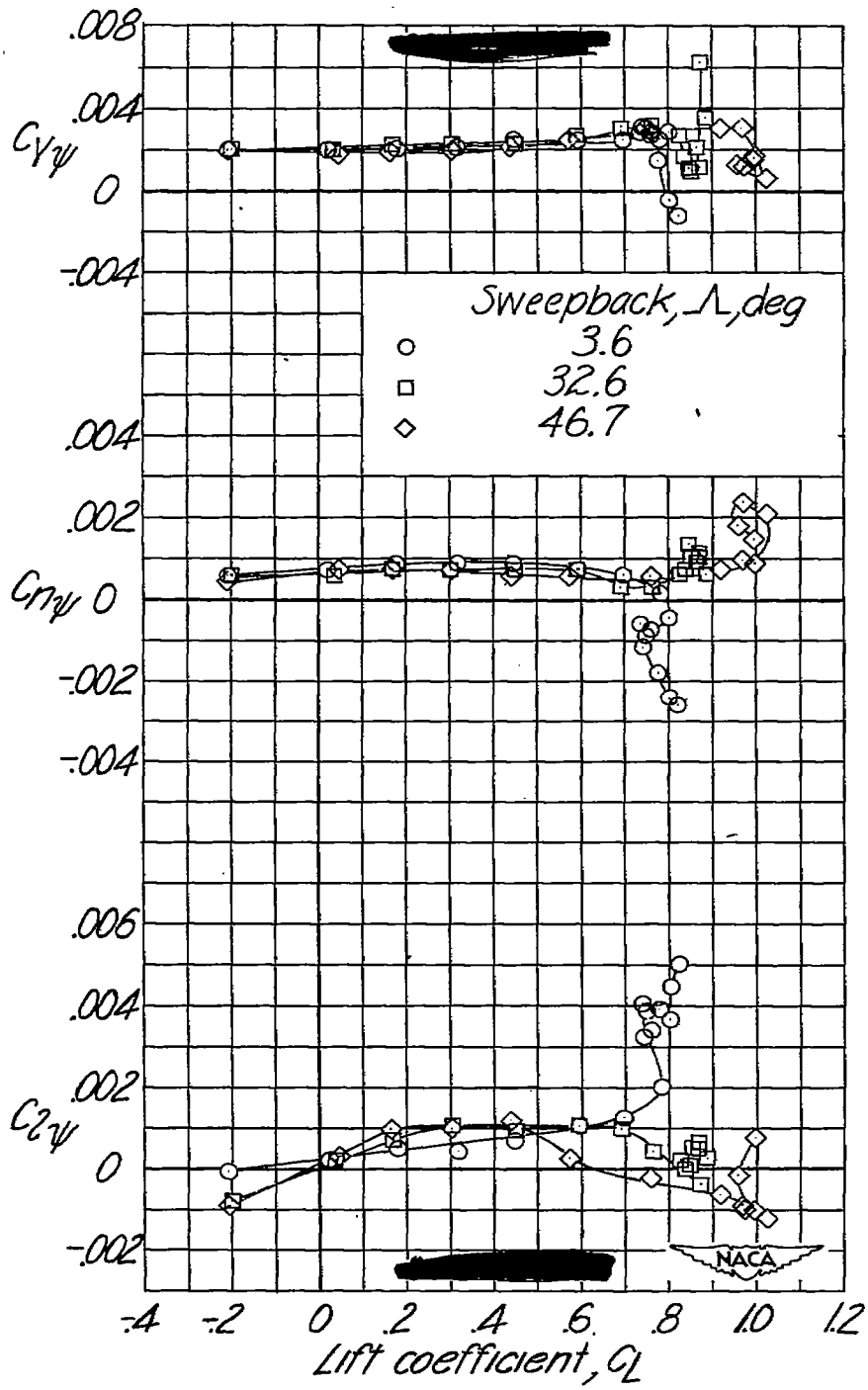

Figure 11.– Variation of C_{Y_ψ}, C_{n_ψ}, and C_{l_ψ} with lift coefficient for the wings tested with a fuselage.

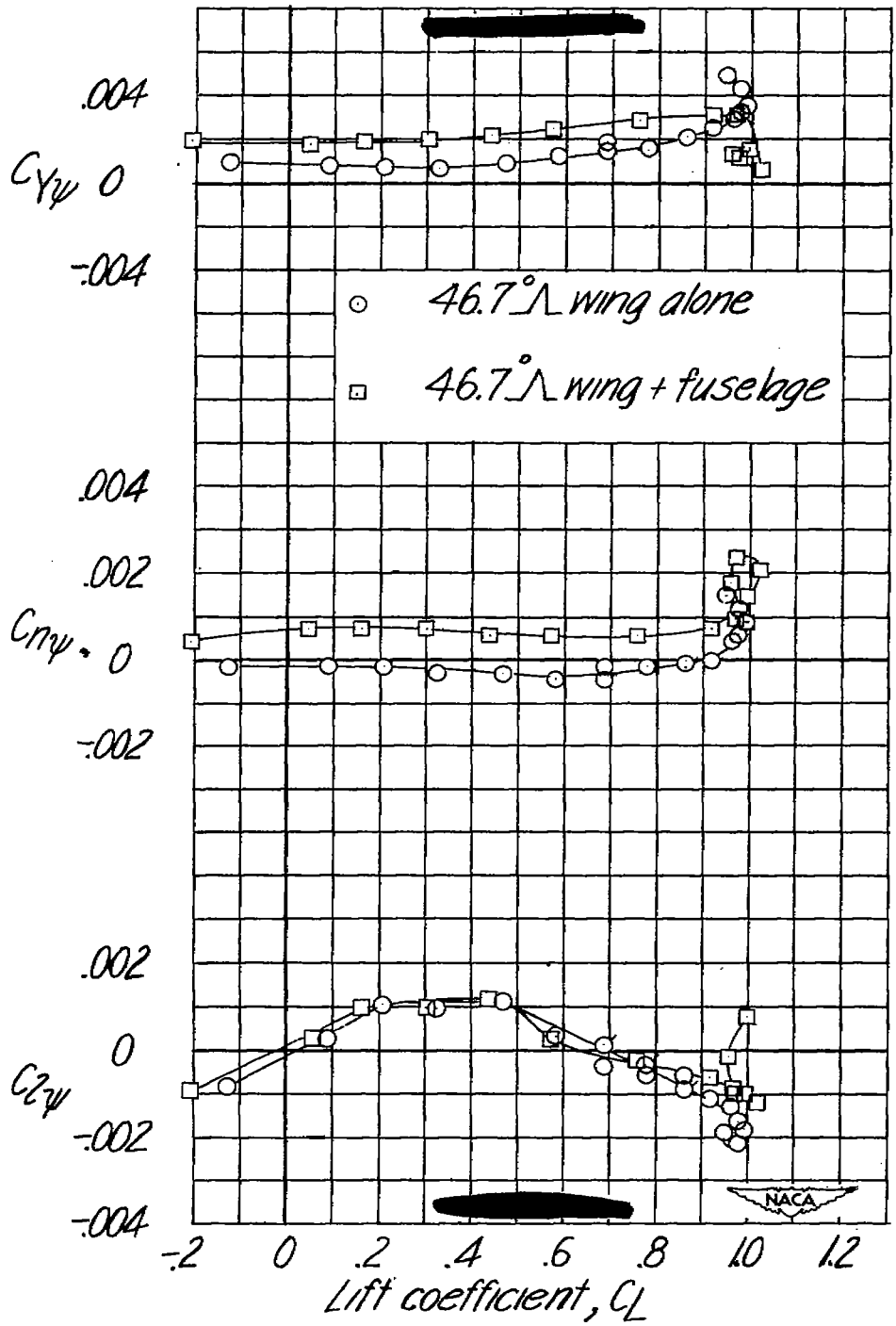

Figure 12.– Variation of C_{Y_ψ}, C_{n_ψ}, and C_{l_ψ} with lift coefficient for the 46.7° sweptback wing tested alone and in combination with a fuselage.

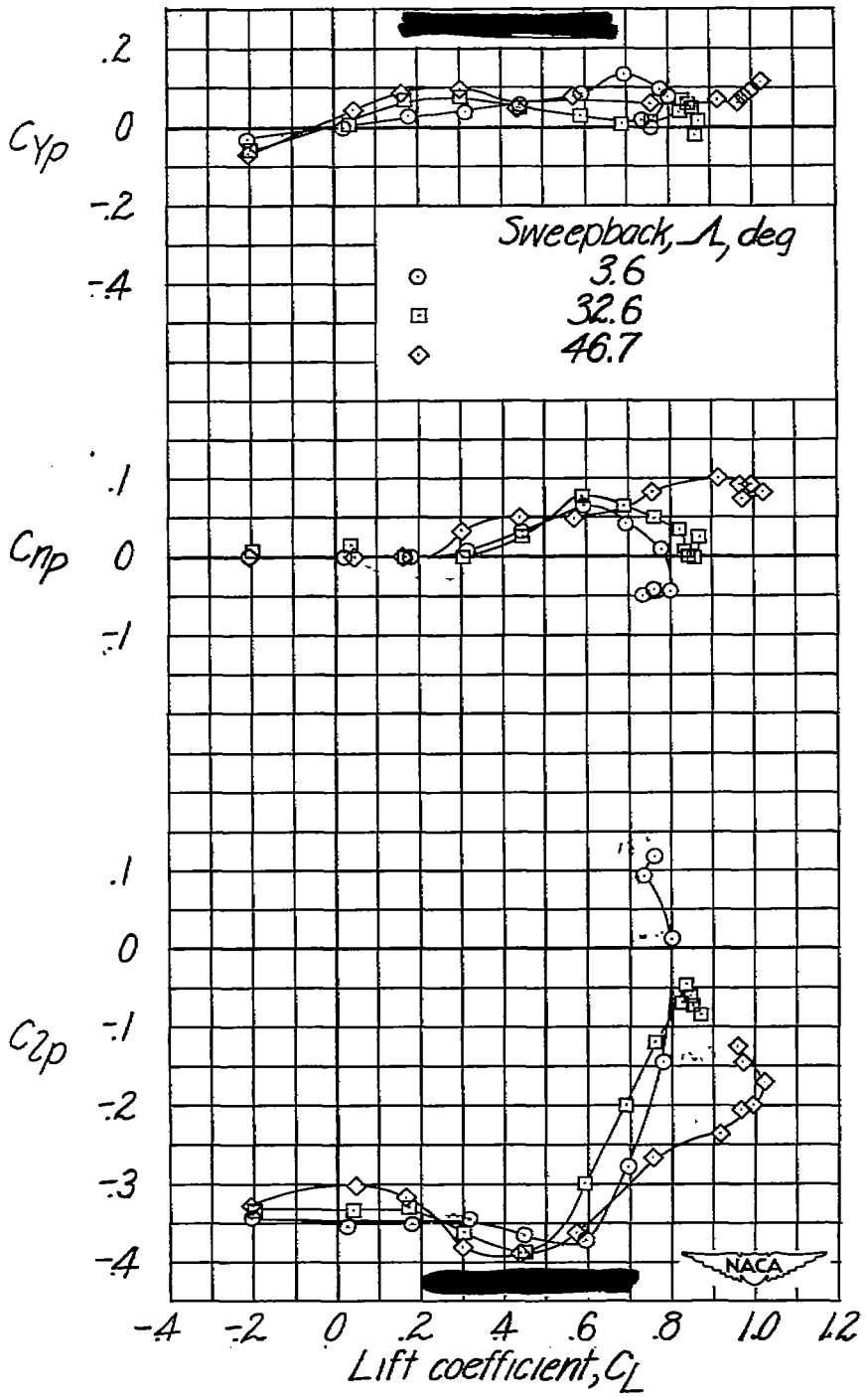

Figure 13.– Variation of C_{Y_p}, C_{n_p}, and C_{l_p} with lift coefficient for the wings tested with fuselage.

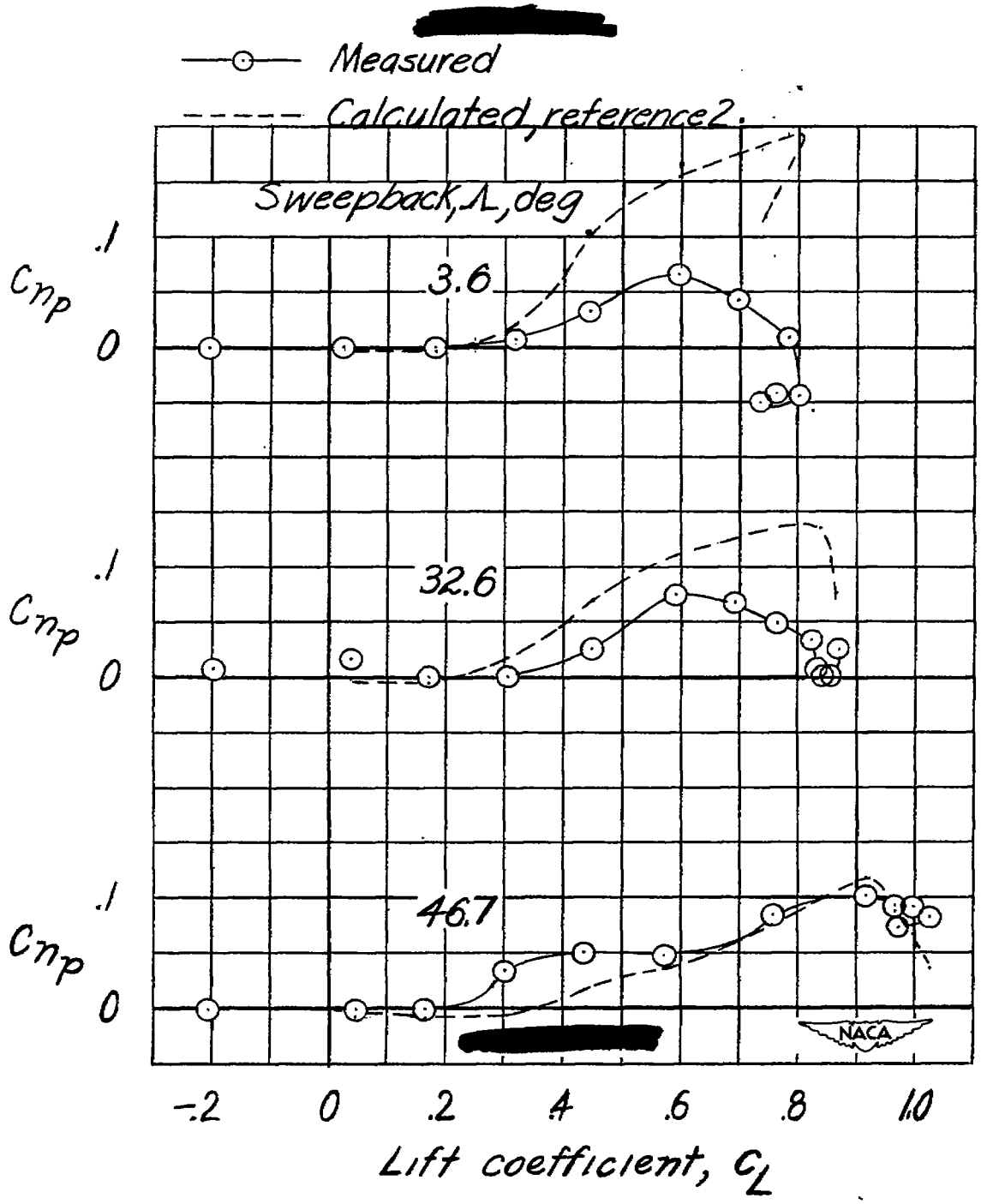

Figure 14.– Comparison of the variation with lift coefficient of the values of C_{n_p} obtained experimentally with those calculated by the method of reference 2.

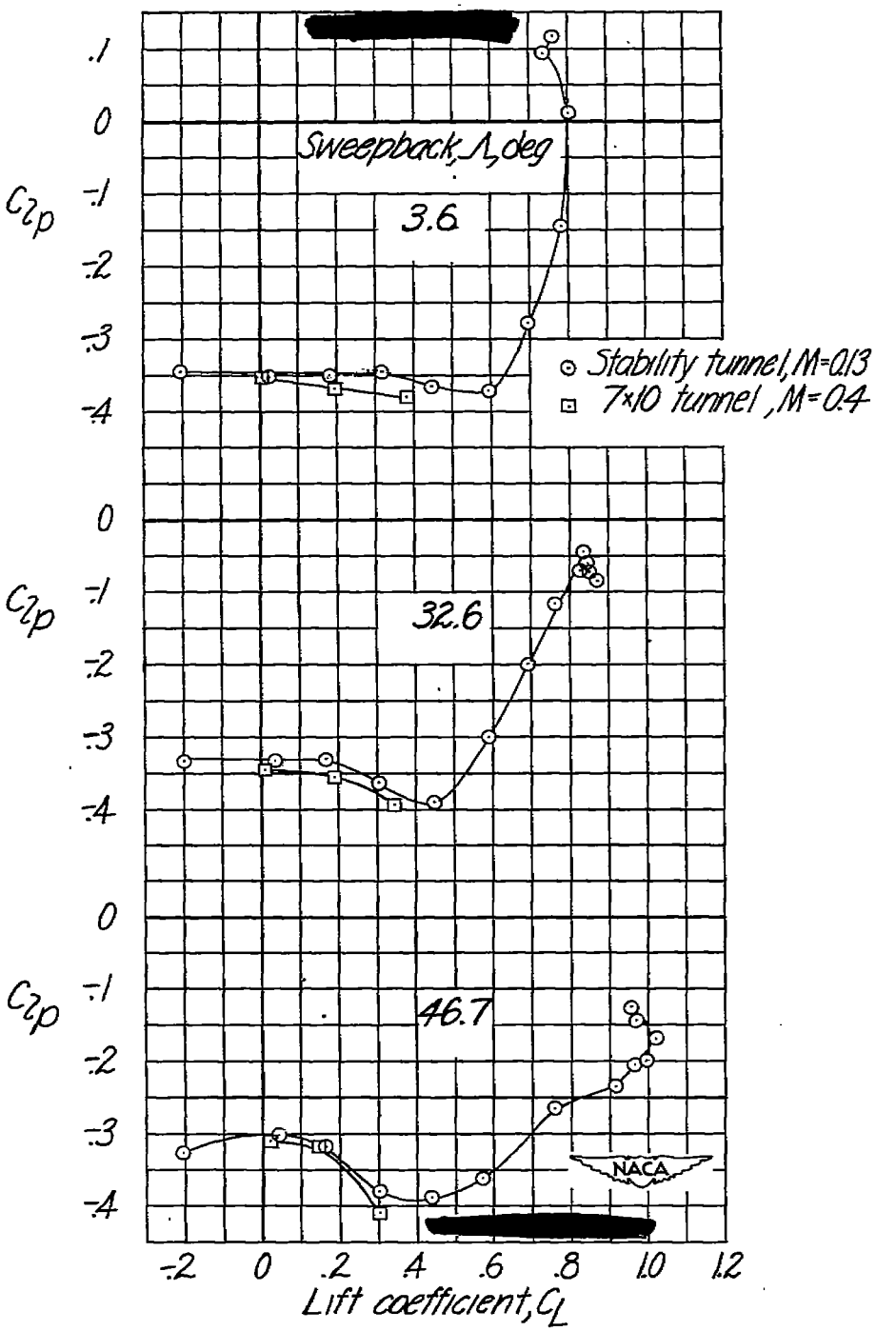

Figure 15.- Comparison of the values of C_{l_p} obtained by free rotation of the models in the Langley 7- by 10-foot tunnel with those obtained by the rolling-flow method in the Langley stability tunnel.

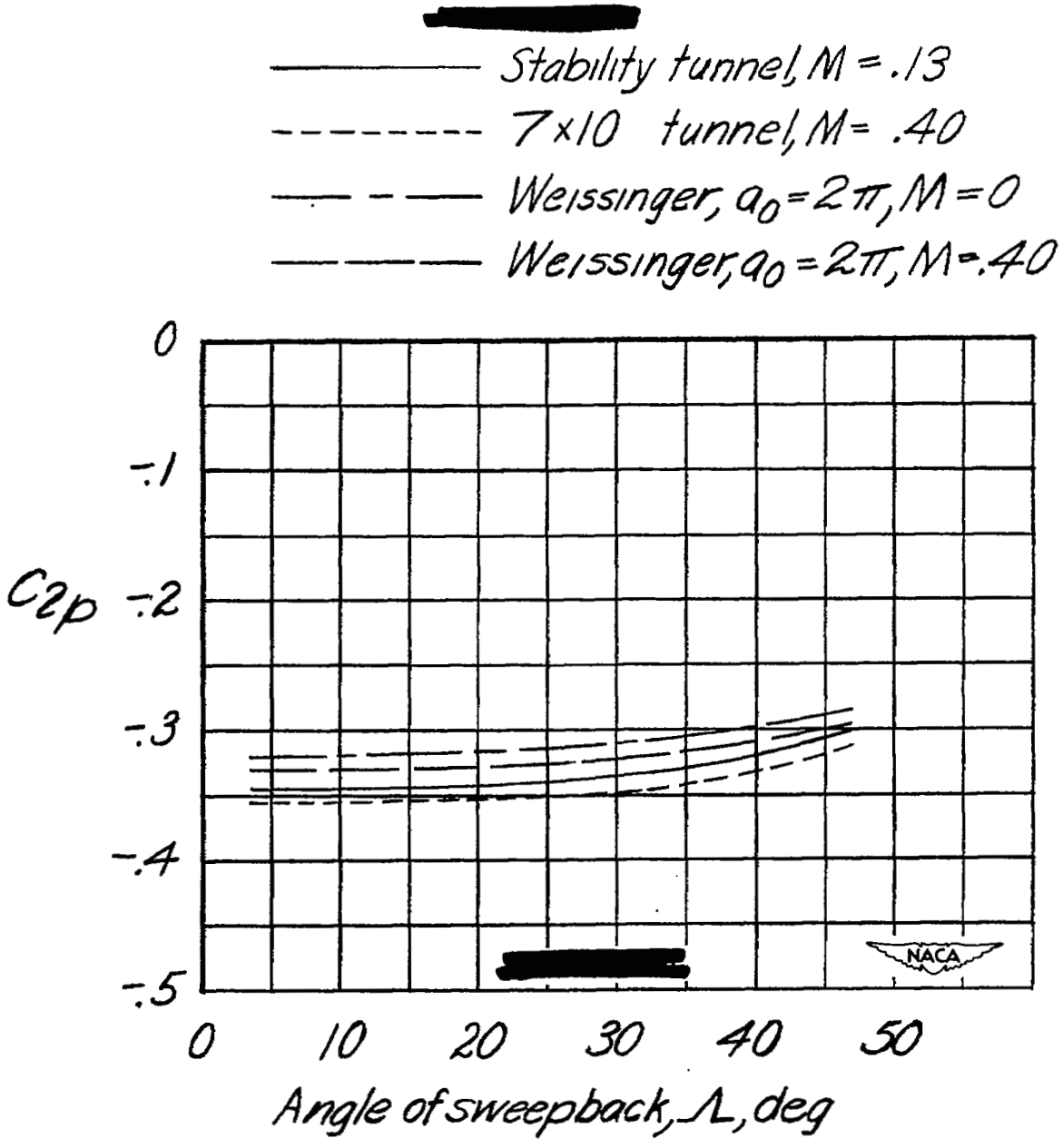

Figure 16.– Comparison of the variation with sweep of the values of C_{l_p} obtained by free rotation of the models in the Langley 7– by 10–foot tunnel and by the rolling–flow method of the Langley stability tunnel with those calculated by the Weissinger method. $C_L = 0$.

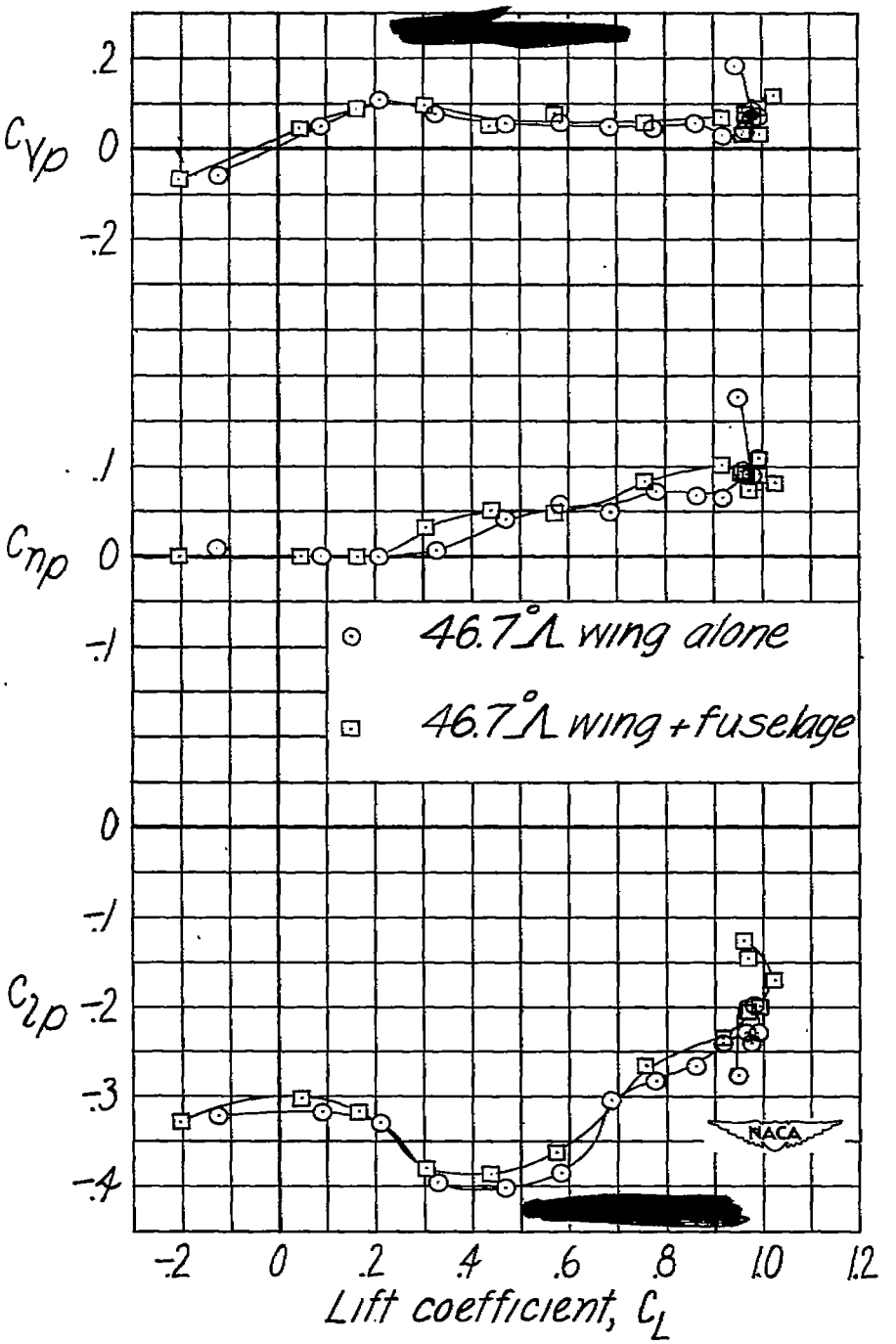

Figure 17.– Variation of C_{Y_p}, C_{n_p}, and C_{l_p} with lift coefficient for the 46.7° sweptback wing tested alone and for the 46.7° sweptback wing tested with fuselage.

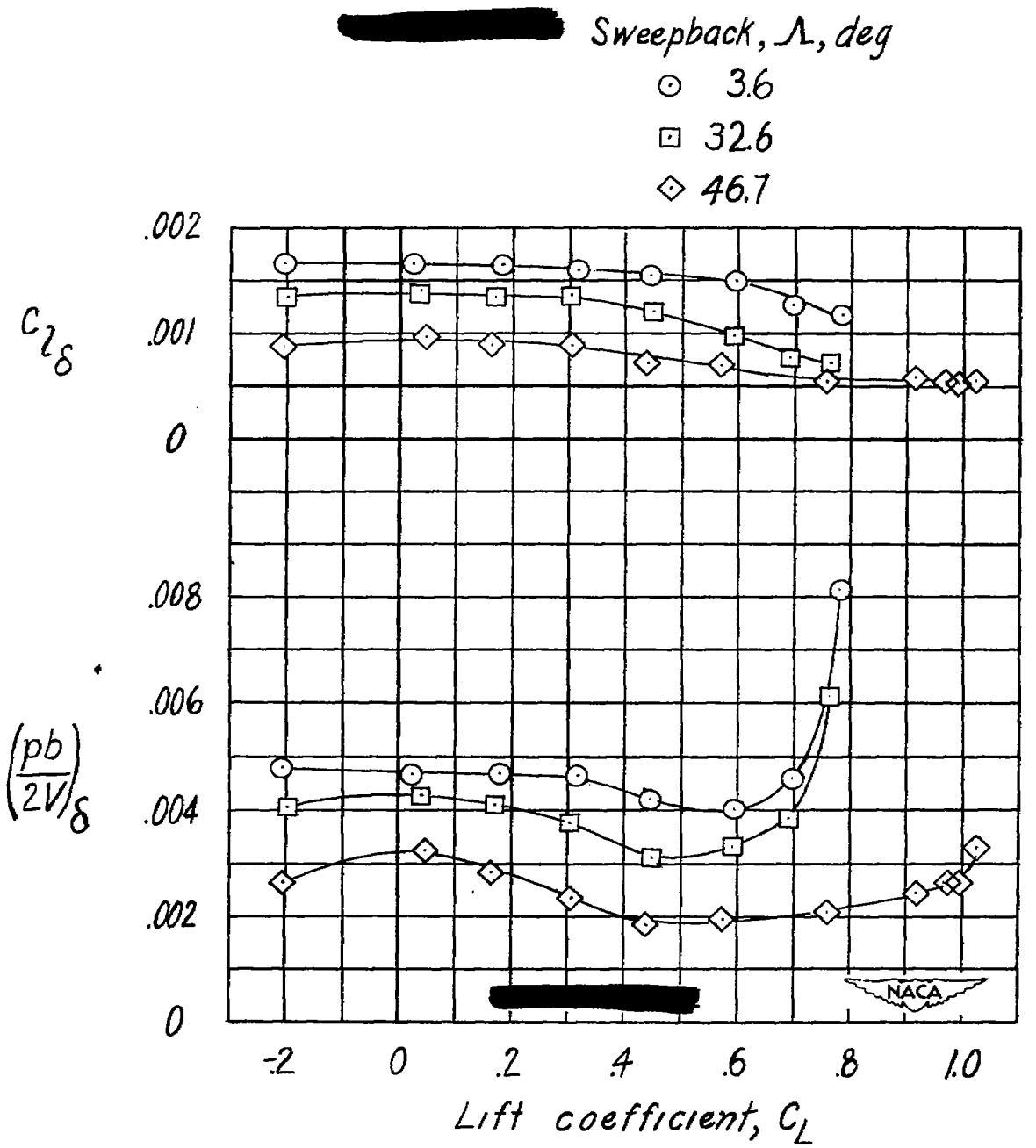

Figure 18.– Variation of aileron effectiveness C_{l_δ} and $(pb/2V)_\delta$ with lift coefficient for the wings tested with fuselage.